DESIGN AND CONSTRUCTION OF A PROTOTYPE RESISTIVE PLATE CHAMBER

by

Zaynab Shahadad Yıldızcı

B.S., Physics, Boğaziçi University, 2016

Submitted to the Institute for Graduate Studies in
Science and Engineering in partial fulfillment of
the requirements for the degree of
Master of Science

Graduate Program in Physics

Boğaziçi University

2019

ACKNOWLEDGEMENTS

First and foremost, I would like to take this opportunity to express my sincere gratitude to my family for always being there for me. To my parents for providing me with the opportunities to become who I am and to get where I stand. Individually to my mom, Hatice Yardım, for her endless love, support and sacrifices to ensure my comfort and happiness. Also to my dad, Erdal Necip Yardım, for being the perfect role model both as a person and as an academic. He guided me through my life, through my education and also through my thesis. He has been like my co-supervisor for this thesis, pursued my progress and held me up whenever I was down, as he always did.

It is equally important to express my gratitude particularly to my husband and also my coworker, Emre Burak Yıldızcı, for his patience and support throughout this process. I cannot thank enough for his intelligent ideas that shaped my understanding of RPCs as well as his help in editing my thesis.

I am deeply thankful to my supervisor Veysi Erkcan Özcan for accepting me as his student and giving me the opportunity to construct a detector from scratch. I am also grateful for his support along the way and for my future academic career.

I owe sincere thanks to my former advisor Evren Özarslan who always supported me, shared his valuable experience and advice.

Lastly, I would like to thank TÜBİTAK for financially supporting me with the 2210-E National Scholarship Programme for MSc Students (2210-E Yurt İçi Yüksek Lisans Burs Programı).

ABSTRACT

DESIGN AND CONSTRUCTION OF A PROTOTYPE RESISTIVE PLATE CHAMBER

Resistive Plate Chambers (RPCs) are gaseous particle detectors that are used in various applications requiring coverage of large volumes with good time and position resolution, such as detection of muons in high-energy physics experiments. We present an overview of the basic literature on RPCs and describe the steps for realizing a modest design with a very limited budget and without the need for a specialized equipment. The details, including information about the materials and their domestic availability as well as the knowhow to resolve encountered issues, are presented with the goal of establishing a baseline for future work on this area. The constructed RPC, which we believe is the first of its kind in Turkey, has been tested with different gases (argon and isobutane) and mixtures (air, argon-air, argon-isobutane). The test results and observations are also presented and their compatibility with the theoretical expectations is discussed.

ÖZET

DİRENÇLİ PLAKA ODASI TASARIMI VE PROTOTİP ÜRETİMİ

Dirençli Plaka Odaları (DiPlO'lar), yüksek enerji fiziği deneylerinde müon algılanması gibi büyük hacimlerin iyi zaman ve konum çözünürlüğü sağlanarak kaplanmasını gerektiren çeşitli uygulamalarda kullanılan gazlı parçacık dedektörleridir. Bu tezde, DiPlO'lar hakkında temel bir literatür özeti sunularak, çok sınırlı bir bütçeyle ve özel donanıma ihtiyaç duyulmadan, mütevazı bir tasarımın hayata geçirilme adımları açıklanmaktadır. Bu alanda yapılacak çalışmalara temel oluşturması amacıyla; malzemeler, bu malzemelerin yerel mevcudiyeti ve karşılaşılan sorunlara getirilen çözüm yolları gibi yapım süreciyle ilgili detaylar sunulmuştur. Türkiye'de türünün ilk örneği olduğuna inandığımız bu DiPlO, çeşitli gazlarla (argon ve izobütan) ve karışımlarla (hava, argon-hava, argon-izobütan) denenmiştir. Test sonuçları ve gözlemler, teorik beklentilere uygunluklarıyla birlikte sunularak tartışılmıştır.

TABLE OF CONTENTS

LIST OF FIGURES

LIST OF SYMBOLS

A	Area
Ar	Argon
b	Resistive electrode thickness
CCl_2F_2	Freon
C_4H_{10}	Isobutane
d	Distance from the primary ionization point
e	Charge of electron
e^-	Electron
E_w	Weighting field
g	Gas gap thickness
ion^+	Positive ion
I	Current
I_{ind}	Induced current
l	Length
m	Insulator sheet thickness
n_0	Number of primary electrons
n_e	Number of electrons
N_2	Nitrogen gas
q	Charge
r	Radius
R	Resistance
t	Thickness
v	Velocity
v_{drift}	Drift velocity
V	Voltage
V_ω	Weighting Potential
x	Distance

α	First Townsend coefficient
α^*	Effective first Townsend coefficient
ϵ_b	Dielectric constant of bakelite
ϵ_{gas}	Dielectric constant of gas mixture
ϵ_{mylar}	Dielectric constant of mylar sheet
η	Attachment coefficient
μ^-	Muon
ρ	Resistivity
Ω	Ohm
$\Omega/\square$	Ohm per square

LIST OF ACRONYMS/ABBREVIATIONS

ATLAS	A Toroidal LHC Apparatus
CERN	European Organization for Nuclear Research
CMS	Compact Muon Solenoid
CNC	Computer Numerical Control
HV	High Voltage
IV	Intravenous Cannula
LHC	Large Hadron Collider
PC	Polycarbonate
PPAC	Parallel Plate Avalanche Counter
PVC	PolyVinyl Chloride
PET	Positron Emission Tomography
RPC	Resistive Plate Chamber
R&D	Research and development
UV	Ultraviolet

1. INTRODUCTION

The adventure of discovering subatomic particles began a little longer than a century ago with J. J. Thomson's experiment with cathode ray tube. In 1897 he discovered negatively charged particles, which have since been called electrons, while observing the deflection of the cathode rays under the influence of an electric field. After his observations he concluded that, since the atom itself is neutral, there must be positively charged particles inside the atom to compensate for the presence of the electrons.

After the discovery of Thomson, Rutherford conducted experiments to better understand the structure of the atom. With the well-known gold foil experiment, in 1908, he observed that the atom has a positively charged center which contains most of the atom's mass. This observation was the discovery of the nucleus and proton. Yet, the nucleus of the atom was unclear. Later, in 1932, a supplemental discovery was made by James Chadwick with the announcement of neutron. The rest of the century was full of continuous discoveries of new particles.

In order to discover highly energetic, short-lived, small sized particles special techniques and devices were needed. This led to the development of accelerators and detectors. With every step of discovery, better devices were developed to acquire more information about the particles such as their energy, lifetime, size, and so on.

First detectors were developed with the image tradition, also called optical method [3,4]. These detectors obtained information via trajectories left by the particles. Operation took place by photographing the trajectory and then analyzing it. Many particles have been discovered by this method; starting with X-rays discovered by Roentgen to the discovery of muons with a cloud chamber by C. Anderson and S. Neddermeyer [3]. Drawback of the optical method was that the data analysis was a tedious task since one has to look at millions of photographs. Without the trigger system, every interaction was to be photographed. Even though valuable position resolution was achieved, be-

cause of the bad rate capability this method needed to be replaced [4]. Hence, optical methods left their place to electrical methods which led to the logic detectors such as Geiger counters and spark counters.

When demand for more information left even the simple electrical methods insufficient, gaseous detectors were introduced. They, in a way, combine the optical and electrical methods providing both good time and spatial resolution. Gaseous detectors utilise the ionization of the gas due to the incident particles and their operation mode is dependent on the magnitude of the applied high voltage (Figure 1.1).

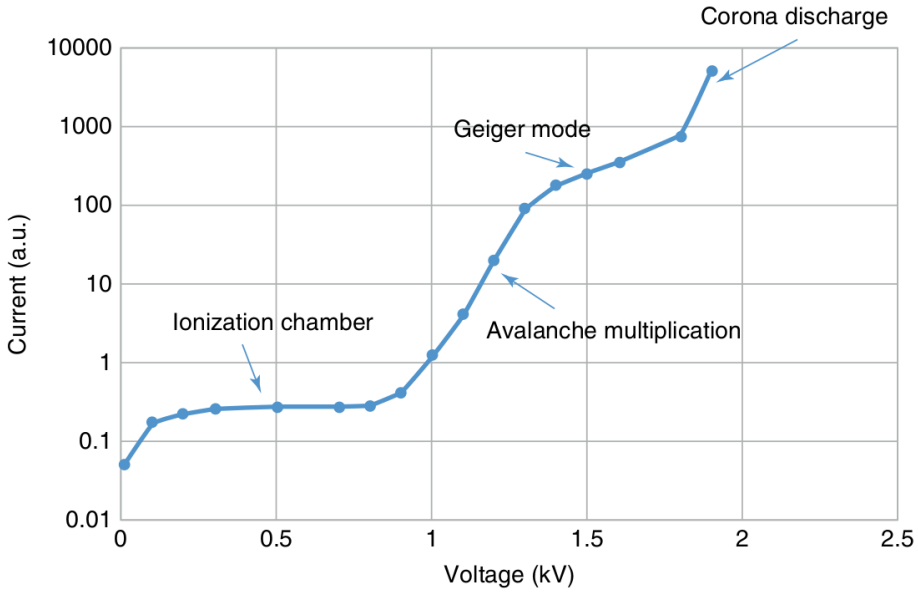

Figure 1.1. Operation modes of gaseous detectors [1].

Resistive Plate Chambers (RPCs), the main topic of this thesis, are gaseous detectors. They operate on the principle of ionization of the gas by highly energetic particles and detection of the signal produced by the drift of these charged particles with the presence of an electric field. They are widely used in various fields due to a number of advantageous features. They are easy to construct, easy to operate and in addition relatively inexpensive compared to other detectors. Details about these features and more about RPCs are discussed in the upcoming sections.

1.1. Historical Developments

In this section, some important steps through the development of detectors those led to the invention of the RPC are introduced. First gaseous detectors had cylindrical geometry. This geometry was preferred because it provides intrinsic advantages. With the cylindrical geometry electric field decreases proportionally with $1/r$, with r being the distance through the inner electrode to the outer electrode. This intense decrease adds a self-quenching mechanism to the detector since the electric field is not intense enough near the outer electrode and a complete spark, therefore discharge, is avoided (Figure 1.2). This is one of the main advantages of the cylindrical geometry. However, this also means an insensitive volume near the outer electrode because the electric field is intense only within a limited volume. Ionized electrons in the outer volume cannot be detected as a result of weak electric field and this affects the efficiency of the detector.

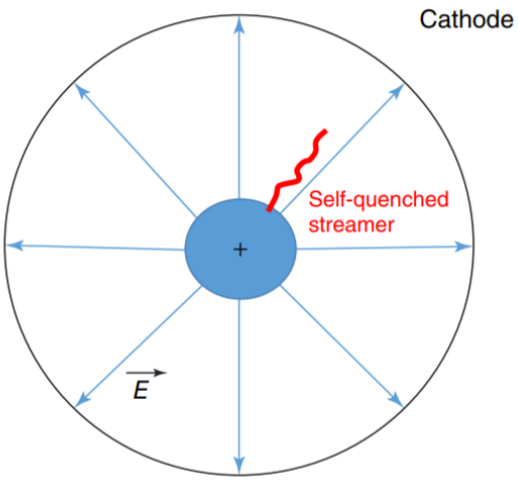

Figure 1.2. Self-quenching mechanism of cylindrical geometry detectors [1].

First constructed cylindrical detector was the Ionization Chamber. Ionization Chambers are used to detect ionizing radiations. Like most of the gaseous detectors its principle of operation relies on the excitation/ionization principle. Metallic electrodes are used in this detector. Drawback of this detector was that it could only respond to relatively high intensity radiation and could not detect a single particle [1]. Being able to detect a single particle was an important issue. To overcome this problem Geiger

counter was developed by Rutherford and Geiger. It uses the electron avalanche principle, which will be explained in detail later, to detect a single elementary particle. This detector also had metallic electrodes and cylindrical geometry. Around 1950s cloud chamber and bubble chamber were introduced. With these devices particle tracking achieved at a single-particle level.

Both metallic electrodes and cylindrical geometry has many disadvantages besides their advantages. These problems are solved step by step. Operating detectors in avalanche mode needs an intense enough electric field (more than a few kV per cm depending on the gas mixture [1]) throughout the whole active area. Since cylindrical geometry lacks this property, as an alternative, planar geometry is introduced. Planar geometry allows a uniform electric field within the detector which enables the avalanche multiplication mechanism throughout the whole detector volume thus, these detectors provide better time resolution. However, planar detectors were not spark protected when they were first introduced.

First parallel plate counters had metallic electrodes [5,6]. These detectors operate in spark mode and they are difficult to build and operate. Although better time resolution than widely used Geiger-Müller Counters is obtained they were not efficient. Both because of the geometry and metallic electrodes, they did not have a self-quenching system and when a localized spark occurred a discharge is formed on the whole detector since the metallic electrodes distribute charges. Therefore these detectors needed a voltage removal, i.e. recovery time, in order to avoid permanent discharge. This means losing a big deal of data with the relatively long dead time thus limited rate capability.

Many attempts has been made to overcome this problem and provide a continuous operation. Since sparks causes this discharge, thus off time, Charpak et al. proposed the operation in avalanche mode in parallel-plate avalanche chambers (PPACs) to overcome this problem [7]. In this mode, the avalanche is obtained with continuous and sufficiently low high voltage (HV). This detector had better rates than the spark counter but still had the problem caused by the metallic electrodes.

Another solution to the discharge problem was presented by Babykin et al. in 1956 [8]. They divided one of the electrodes into small sections, which were insulated from each other, and connected each section to voltage sources through high resistances in order to localize and quench the spark.

An alternative to the metallic electrodes was suggested in 1971 with the introduction of resistive electrodes [9]. These planar spark counters, which were later named Pestov Counters, had one resistive and one metallic electrode thus the occurred spark was not distributed over the resistive electrode. With this feature, detectors with planar geometry acquired an internal quenching mechanism. After a period of its R&D, Pestov Counters achieved good time and position resolutions [10]. However, the design criteria, including a high gas pressure and a narrow gap width, were strict and the construction steps were very tedious.

Santonico et al. came up with an almost perfect solution. In 1981, they introduced Resistive Plate Counter as they called it at that time [2]. The detector was later named Resistive Plate Chamber.

1.2. Fundamentals of RPC

RPCs are often used for muon detection purposes and they have different designs for different needs e.g. single gap, double gap, multi gap, timing, and so on. While having different designs, all have the same basic working principle. We constructed the simplest version, a single gap RPC and the rest of the section is about this simple single gap RPC as it was first introduced in [2].

As Santonico et al. presented, this new detector, RPC, is the improved version of the Pestov Counter [11] with many simplifications in both construction and operation [2]. RPC's are highly efficient detectors with good time resolution (97% efficiency with about 1 ns time resolution) and since they are easy to construct with low cost they are good candidates for large area detection. The layout of the first RPC can be seen in Figure 1.3.

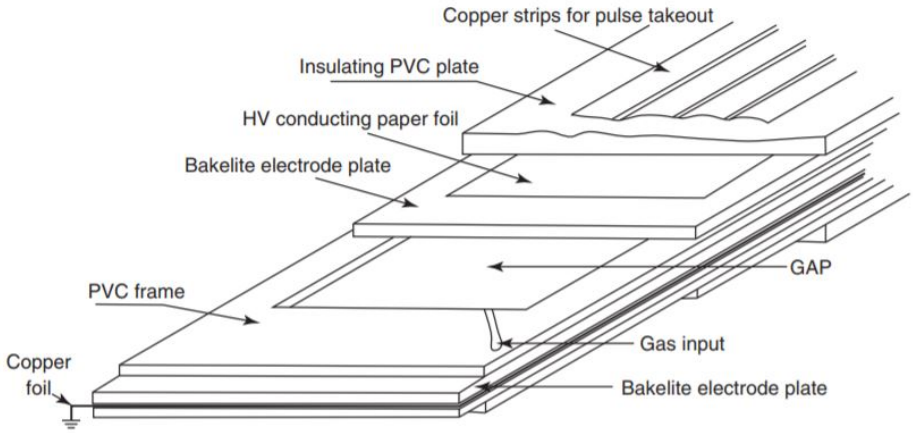

Figure 1.3. Layout of the first RPC prototype [2].

RPC's planar geometry provides many advantages in resolution since the electric field produced is uniform throughout the gas gap whereas in cylindrical geometry it decreases proportionally with $1/r$ from the center. However, as mentioned before, planar counters do not have a self-quenching mechanism that cylindrical ones have. This problem is solved in RPCs. They are built with resistive electrodes. In the first prototype, a plastic-like material called bakelite, highly resistive material made of resin, is used for this purpose. With the resistive electrodes discharge is not distributed over the electrode, it is localized [2]. This characteristics improves the rate capability of the detector since the detector does not need a shut down, i.e. HV removal, for recovery which provides continuous operation opportunity for the detector, thus, it can respond to intense beams. This is one of the main reasons why RPC's are suitable for large area detection experiments.

Another important property of this detector is that it can operate both in streamer mode and avalanche mode determined by the number of ionized electrons. This number, therefore the operation mode, is dependent on the gas used and the applied high voltage [12]. RPCs are generally operated in avalanche mode since it provides a better rate capability [13]. These avalanche and streamer modes will be explained in detail later. For an RPC to function in avalanche mode, a gas that has UV absorption property must be added to the active gas to avoid secondary discharges. In the first

prototype and generally in RPCs this active gas is argon (Ar). For UV absorption, isobutane (C_4H_{10}) has been used commonly. It is good to mention here that the operation of RPCs are conducted at the atmospheric pressure which is a feature of an easy operation.

While the electrode resistivity and the gas mainly determines the rate capability, the gas gap width determines the time performance [14]. The gas gap is usually 2 mm in RPCs, but timing RPCs have smaller gaps. This gas gap is formed by gluing insulating spacers between the two electrodes. In addition to edge spacers multiple smaller spacers are uniformly distributed inside the detector to hold the gas gap stable and keeping the electrodes same distance apart. Stability of the gas gap is important to provide a uniform electric field across the whole detector. It is also important to avoid dust inside the gas gap. Electrodes must be smooth and cleaned for improved efficiency. As mentioned above, uniform electric field is important for better spatial resolution since its effect must be the same for all events.

In order to produce an electric field through the resistive electrodes, some adjustments are needed to be made. There is a need for a conductive material to apply voltage to the electrodes. Also this material must be uniformly spread over the electrodes for the production of the uniform electric field. For this purpose Santonico et al. glued a copper foil on one electrode and a conductive paper to the other for the first prototype [2].

This first prototype was 103×22 cm^2 in size with 1.5 mm gas gap and it could be operated with 10 kV voltage difference with no need for signal amplification. Signal readout is performed with copper strips which are isolated with PVC from the high voltage.

Until now information provided about RPCs are generally based on the first prototype. Since RPCs were very promising, further researche have been done for its improvement. For instance, after the first introduction, in 1988, slight improvements are introduced to show compatibility for large area detection with a time resolution of

the order of 1 ns [15]. In this paper, total area of 5.8×0.48 m^2, double gap RPC is introduced. Also, a new gas mixture is introduced to improve the operation in avalanche mode. In addition to the active and the UV absorption parts, electronegativity is added to the gas mixture with the addition of a small amount of freon (CCl_2F_2). It is important to remind here that a change in the gas mixture requires the adjustment of the electric field hence the operation voltage. Another improvement in this RPC was that semiconductive surface was obtained by graphite paint instead of using a copper film and a semiconductive paper. Using graphite paint enables one to adjust the conductivity to the desired amount. Order of magnitude of the conductivity is important, it should not be too high or too low. When the conductivity is not high enough, high voltage could not spread uniformly over the surface resulting nonuniform electric field. When it is the opposite, the signal is shielded and cannot be obtained from the readout panel.

It has been 38 years since the first introduction of the RPC. Thanks to the systematic studies and wide usage of RPCs they have been improved significantly. Two largest experiments conducted at CERN, ATLAS and CMS, use RPCs since they can respond to intense beams. In reference [12] a late version of RPCs used in ATLAS experiment is introduced. Substantial difference in these new RPCs is the gas mixture. One of the main considerations for choosing the gas mixture is its environmental impact. Some gases are harmful to the environment and they need to be replaced with eco-friendly ones. Finding an eco-friendly gas mixture is one of the main research areas of RPCs and there are numerous studies being conducted [16, 17].

In addition to the high-energy physics experiments RPCs are used in many other fields. Medical imaging devices have enormous importance in our lives. Being able to detect what is happening inside a body without cutting it open or, figuring out a defected tissue early enough to take precautions is important as the life itself. Positron Emission Tomography (PET) is one of the most important imaging modalities since it can display very depths of our body. To further develop the PET, studies of the usage of RPCs along with the PET are being conducted. Spatial and time resolutions are very important in imaging modalities for the image quality, therefore, high time

resolution of RPCs make them very powerful candidates for this task [1].

Lately, prototype of a new device to further benefit other fields has been built using RPCs. This new device uses cosmic muons to detect cavities inside any constitution, for example hidden chambers inside a pyramid or an undiscovered cave inside a mountain which will be beneficial for new archaeological and geological discoveries [18].

2. THEORY

2.1. Avalanche Formation

Everything starts with a muon or in general a highly energetic particle producing a primary electron as a result of colliding with a gas atom or a molecule while passing through the gas gap. Ionization process of muon is shown in Equation 2.1.

$$\mu^- + atom \rightarrow \mu^- + ion^+ + e^- \tag{2.1}$$

This produced primary free electron accelerates under the influence of an electric field between the electrodes and gaines energy. If the electric field is intense enough for the electron to reach the energy level required to further ionize an atom, second electron will be ionized. This process continues consecutively with the exponentially increasing number of electrons in each step and this is called avalanche multiplication, first discovered by John S. Townsend [19]. These consecutive ionizations originating from the primary electron form an electron avalanche. Schematic illustration of this process can be seen in Figure 2.1. Size of this avalanche depends on the magnitude of the electric field, width of the gas gap and the gas mixture filling the gas gap.

Infinitesimal increase in the number of electrons in an avalanche is given by the Equation 2.2.

$$dn_e = n_e \alpha dx \tag{2.2}$$

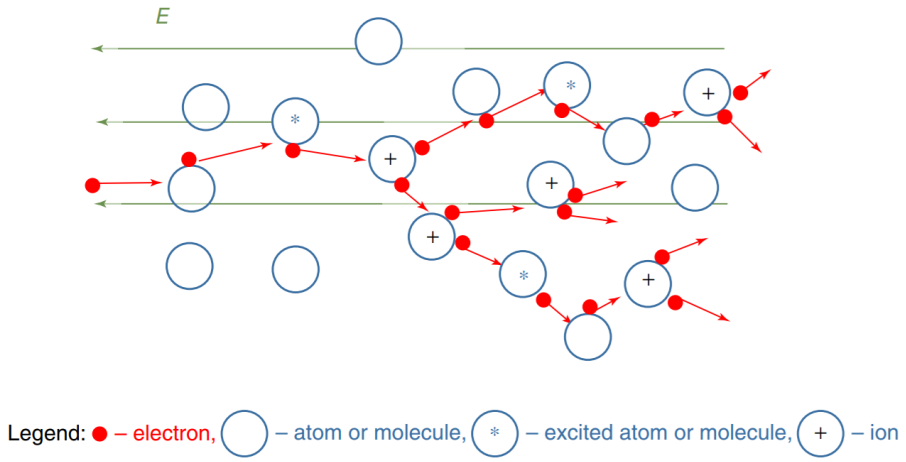

Figure 2.1. Illustration of the electron avalanche [1].

Here, n_e is the number of electrons, is the first Townsend coefficient and x is the direction towards the anode electrode. The effect of the electric field and the gas mixture is included in α. From integrating Equation 2.2, we obtain

$$n_e = n_0 e^{\alpha d} \tag{2.3}$$

where n_0 is the number of primary electrons and d is the distance from the primary ionization point, along the x-axis.

2.1.1. Avalanche to Streamer Transition

There is a limit to the number of electrons can be in an avalanche. When the electrons inside an avalanche reaches to the limit of approximately 10^8 electrons, it loses its avalanche properties and turns into a streamer (Figure 2.2). This limit is called the Reather Limit [20]. When the streamer forms, it produces a discharge between the anode and cathode. As mentioned before, operating in streamer mode severely decreases the rate capability. In order to avoid the formation of a streamer,

i.e. to restrain the growth of an avalanche, electronegative and UV absorber gases are added to the active gas. Effect of these gases on the avalanche is explained respectively.

2.1.2. Effect of the Electronegative Gas

Electronegative gas atoms have a tendency to become negatively charged. Thus, when a free electron moves in a gas mixture in which an electronegative gas exists, there is a probability of an electronegative gas atom to capture the electron and become a negative ion. This process reduces the number of free electrons in the gas mixture hence the avalanche size is reduced. The infinitesimal decrease in the number of electrons in an avalanche due to the electronegative gas is given by

$$dn_e = -n_e \eta dx \tag{2.4}$$

where η is the attachment coefficient.

To account for both ionization and attachment effects, the effective first Townsend coefficient α^*, which is defined as $\alpha^* = \alpha - \eta$, must be introduced and Equations 2.2 and 2.3 become

$$dn_e = n_e \alpha^* dx \tag{2.5}$$

$$n_e = n_0 e^{\alpha^* d} \tag{2.6}$$

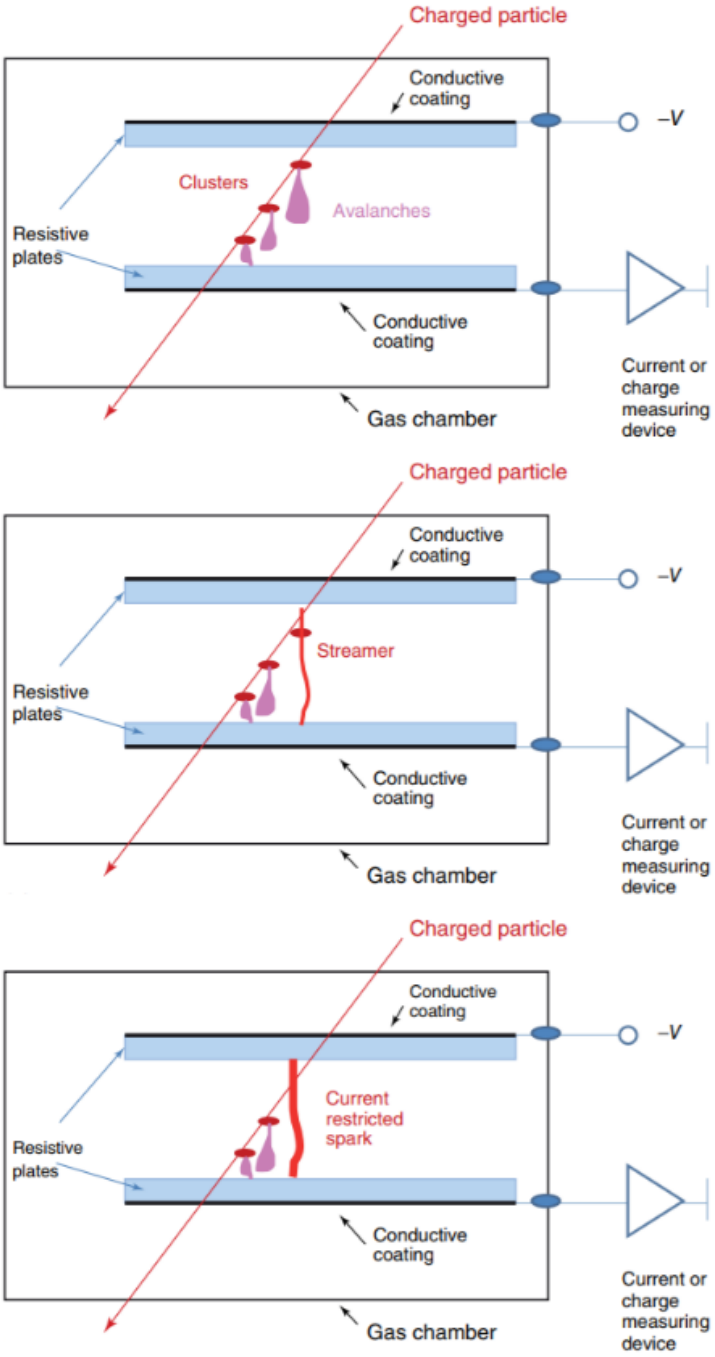

Figure 2.2. Avalanche to streamer transition [1].

2.1.3. Effect of the UV Absorber Gas

Like the electronegative gases, UV absorber gases also have an effect of decreasing the number of free electrons in the gas mixture. As the particles, both electrons and muons, move inside the gas gap they lose energy. One of the main mechanisms that causes the energy loss is their collision with the atoms. These collisions result in ionization or excitation of the atoms. When an atom is excited, it goes through the process of de-excitation in a short period of time. Some of the atoms in that process emit UV photons that have enough energy to further ionize the gas, therefore increase the number of free electrons inside. These new free electrons may either join in an avalanche or potentially create new avalanches [21]. To capture the UV photons a UV absorber gas must be added to the gas mixture.

2.1.4. Other Effects

There are many other effects that may be taken into consideration that affects the avalanche size depending on the gas mixture but most of them are negligible. Here, two of the more important effects are introduced.

First one is the Penning Effect [22]. This effect can be observed in particular gas mixtures including a gas that has higher metastable energy level, call it gas A, than ionization energy of the other gas, gas B. Penning effect increases the number of electrons as a result of the ionization of the gas B by colliding with the gas A that has an electron at a metastable energy level. The electron of gas A gives its energy to the electron of B while de-exciting. Electron of gas A is de-excited with the collision instead of photon emission since it is in a metastable state.

The other relatively important effect is the detachment effect. This effect is the opposite of the attachment effect. Here, negative ions give the excess electron to the gas mixture and increase the free electron number.

2.2. Signal Development

The electrons that are drifting towards the anode, whether they form an avalanche or a streamer, do not reach the pick-up strips. They are neutered inside the gas gap once they reach the resistive bakelite plates. So the signal is not acquired directly from these electrons but as a result of their movement inside the gas gap. The layers between the gas gap and the readout strips are the resistive electrode, semi-conductive graphite paint and Mylar sheet respectively. They are all resistive materials which makes them transparent to the induced signals stems from the motion of the electrons. Copper strips are placed after the insulating Mylar sheet for the acquisition of the induced signal. Since copper is a metal, there are many free electrons inside the copper strips. The drifting electrons in the gas gap, depending on their drift direction, either repel or attract those free electrons. Assuming the electrons are drifting towards the lower copper strips, they will repel free electrons on the lower strips and through the copper strips to the ribbon cables where the signal will be acquired by the front-end electronics. While the electrons are drifting towards the lower strips they are also drifting away from the upper strips, thus, the free electrons in the upper copper strips will be attracted towards them. So, the expected readout signals from the upper and lower panels must be the exact opposite of each other. For the expected value of this signal Shockley-Ramo Theorem can be used.

2.2.1. Shockley-Ramo Theorem

W. Shockley [23] and S. Ramo [24] introduced a simple approach and derived a simple expression for the induced current on a conductor caused by a moving charged particle. For this method to be applicable, all of the conductors must be grounded to not affect the induced current. Then, to compute the induced current on a particular conductor they introduced a hypothetical electric field, later called Weighting Field, which is equal to the value of the electric field that would occur at the instantaneous position of the point charge when it is removed and the potential of the conductor which we will measure the induced current is taken as unit potential. The simple expression for the induced current is

$$I_{ind} = qE_w v \tag{2.7}$$

where q is the total charge, E_w is the weighting field and v is the velocity of the charge.

According to this formula, to find the induced current on a conductor one has to find the Weighting Field, E_w which is a straightforward task for RPC because of its planar geometry. Considering the strips as infinite parallel plate conductors and keeping in mind that for infinite conductive parallel plates separated from each other by a distance d, we have

$$V = Ed \tag{2.8}$$

where V is the potential difference between the plates and E is the uniform electric field.

Thus, the expression for the strip closest to the electron avalanche, ignoring the thin graphite and glue layers, is

$$\frac{E_w}{\epsilon_b} 2b + \frac{E_w}{\epsilon_{gas}} g + \frac{E_w}{\epsilon_{mylar}} 2m = V_w \tag{2.9}$$

where ϵ_b, ϵ_{gas}, ϵ_{mylar} are the relative dielectric constants of bakelite plates, gas mixture and Mylar sheets respectively and b,g,m are their thickness respectively. Here, since we take the potential of one conductor as unit potential, V_w should be unity. Then, taking ϵ_{gas} to be 1, we have

$$E_w = \frac{\epsilon_b \epsilon_{mylar}}{2b\epsilon_{mylar} + 2m\epsilon_b + g\epsilon_{mylar}\epsilon_b} \tag{2.10}$$

Therefore, by combining Equations 2.7 and 2.10, we have the following expression for the induced current I_{ind}

$$I_{ind} = n_e e \frac{\epsilon_b \epsilon_{mylar}}{2b\epsilon_{mylar} + 2m\epsilon_b + g\epsilon_{mylar}\epsilon_b} v_{drift} \tag{2.11}$$

While calculating the induced signal for the RPC, only the motion of the electrons is considered instead of the motion of all charged particles that are drifting, i.e. electrons, negative ions and positive ions, despite the fact that the number of positive ions is of the same order of magnitude as the number of electrons. The reason for this is that the induced signal is proportional to the drift velocity and the drift velocity of ions is much lower than of electrons.

3. CONSTRUCTION OF 10×15 cm^2 RPC

We have constructed an RPC 10 cm in width, 15 cm in length and around 7 mm in thickness in total as sketched in Figure 3.1. As in the first prototypes of RPC [2] we used bakelite plates as our resistive electrodes and polycarbonate plates as our spacers. Before starting to assembly the RPC, it is important to check the material properties for the operational convenience.

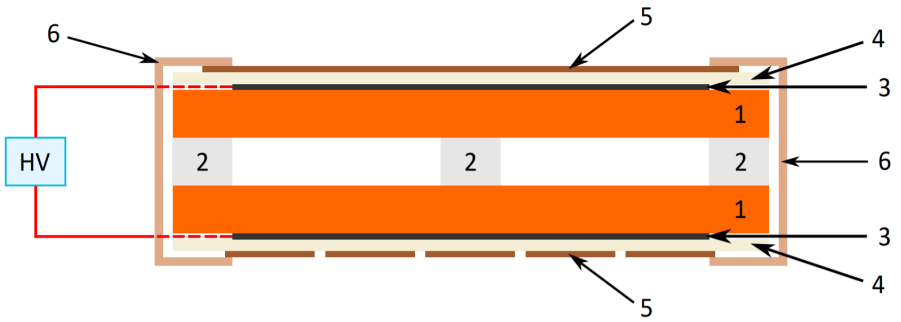

Figure 3.1. Schematic layout of our design of the prototype RPC. 1-Bakelite electrodes. 2-PC spacers. 3-Graphite layers. 4-Mylar sheets. 5-Readout strips lying on the x and y axis. 6-Kapton tapes.

3.1. Bakelite Electrodes

We decided to obtain 2 mm thick Chinese bakelite plates since it is the common thickness. They can be seen in Figure 3.2. Since we knew our resistive electrodes must have bulk resistivity between $10^9 - 10^{12}$ Ω cm [12], as the first step we measured their bulk resistivity to check whether they are suitable for our needs or not. For this task we used Ohm's Law:

$$V = I \times R \tag{3.1}$$

where V is the voltage across the bakelite plate, I is the current passing through it and R is the resistance. From R, bulk resistivity of the bakelite plate can be found using

$$R = \rho \frac{l}{A} \tag{3.2}$$

where ρ is the resistivity, l and A are the dimensions of the plate.

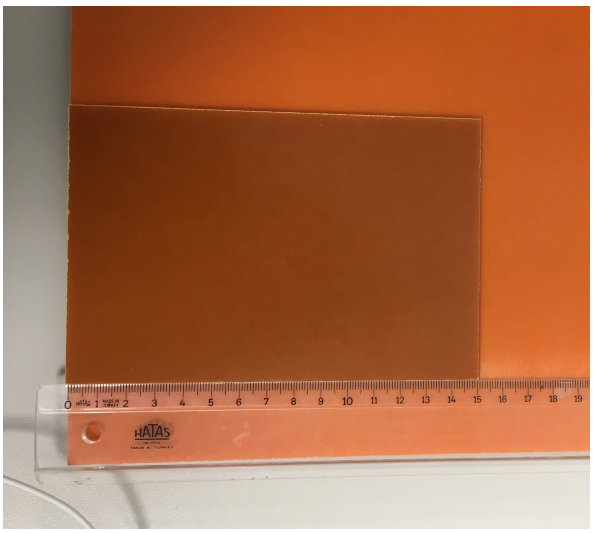

Figure 3.2. Bakelite plate.

Two ends of the bakelite plate were covered with aluminum strips to provide a uniform voltage difference across the two ends. Then we connected one of the strips to the high voltage source while connecting the other to ground. We also connected a multimeter in series to the circuit as an ammeter and read the current from the multimeter while changing the voltage from the source. Our circuit can be seen in Figure 3.3. Then we plotted the corresponding values to the $V - I$ graph and calculated the bulk resistivity of our bakelite from the slope of the $V - I$ graph to be $(0.753 \pm 0.029) \times 10^9\ \Omega$ cm. The graph and the values of our measurements can be found in Figure 3.4. This result confirms that our bakelite electrodes were suitable for our needs.

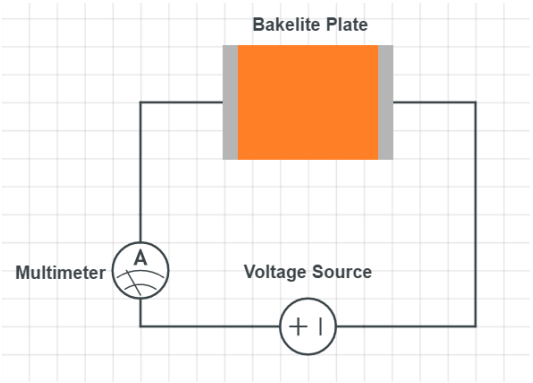

(a) Schematics of bakelite plate bulk resistivity measurement circuit.

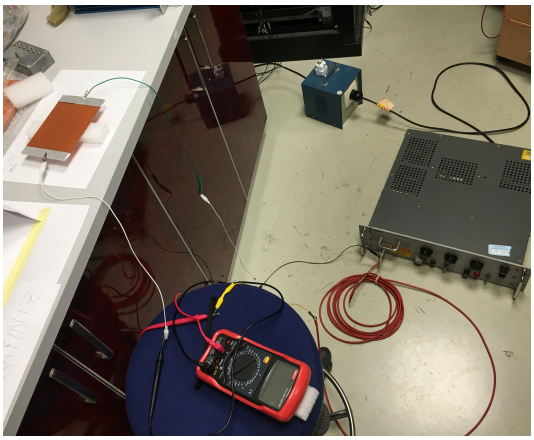

(b) Bakelite plate bulk resistivity measurement setup.

Figure 3.3. Bulk resistivity measurement.

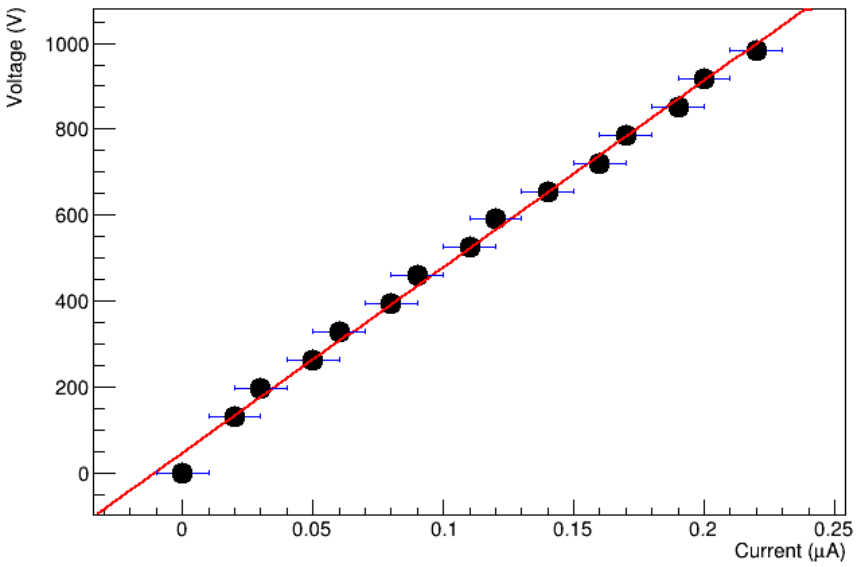

Figure 3.4. Graph of the bakelite bulk resistivity measurement.

3.2. Polycarbonate Spacers

A polycarbonate (PC) plate was needed for making the insulating spacers to be placed between the resistive electrodes to form the gas gap and hold it uniform for the formation of the uniform electric field between the electrodes. Gas gap width is chosen to be 2 mm since it is the most suitable choice for a single gap RPC [25, 26]. So, a 2 mm thick polycarbonate plate was procured from a domestic supplier, Polikarbon.

We decided to use frame-shaped spacer as the edge spacer in order to avoid any possible gas leakages between edge spacers. Since an inside spacer is needed every 10×10 cm^2 to prevent the resistive electrodes from bending towards each other when high voltage is applied and to hold the gas gap stable, we decided to use two 1 cm diameter button spacers placed symmetrically inside the gas gap since our prototype was small in size.

PC is a tough material so, cutting it smoothly with precise measurements needed a special method. An advertisement company, Gramofon Reklam, cut the spacers from our PC plate with a CNC machine. Two holes needed to be drilled through the edge spacer for the gas inlet and outlet and since the gas gap would be 2 mm thick our holes needed to be smaller. This scale of a hole was hard to achieve. There was also another problem, our gas holes were small for standard gas nozzles, so we needed a connector in between the holes and the gas tank. What we needed to do was to find a possible connector, i.e. gas nozzle, and drill the hole accordingly. In short, we needed a small diameter nozzle, like a needle, that could be connected to the gas tank with a pipe and also the system must be leak-proof. In hospitals infusion is transferred into the vein with a needle and through a pipe which was a system quite similar to what we needed. The needle is called the intravenous cannula (IV) (Figure 3.5(a)) and the pipe that connects it to the infusion bag is the infusion set (Figure 3.5(b)). Since they are designed to prevent liquid leakage they were good candidates to prevent gas leakage. Smallest IV had 0.6 mm diameter and we decided to use it as our gas nozzle. Then to have the edge spacer drilled for gas holes we took it to a jewellery atelier since they do similar handiwork with the jewellery and had our PC edge spacer

pierced there. 0.6 mm diameter gas nozzle holes through the edge spacer 3 cm from the corners are obtained. The holes were on the opposite corners to provide a better gas circulation. With obtaining our gas holes, our spacers were now ready for construction of the skeleton of the RPC (Figure 3.6).

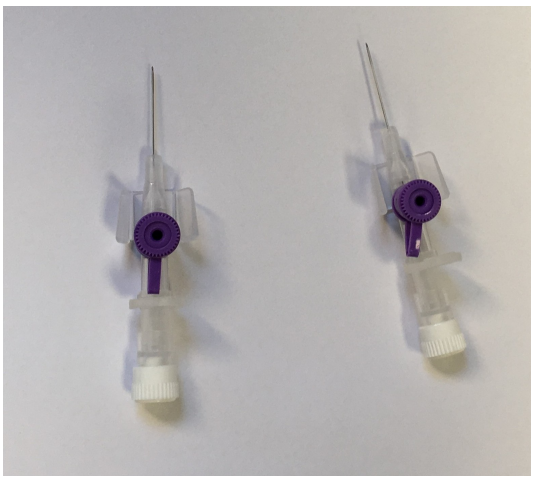

(a) Intravenous cannula.

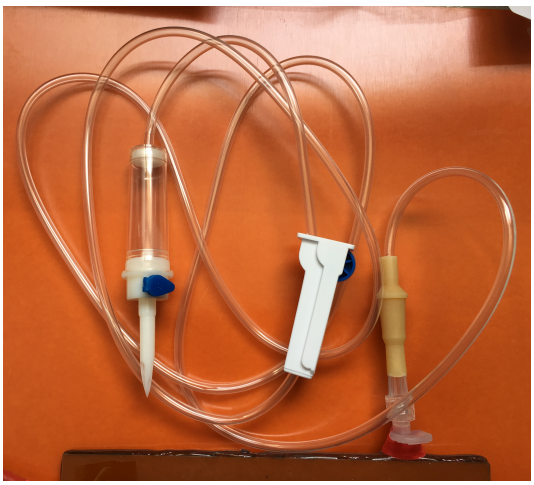

(b) Infusion set.

Figure 3.5. Gas transfer system.

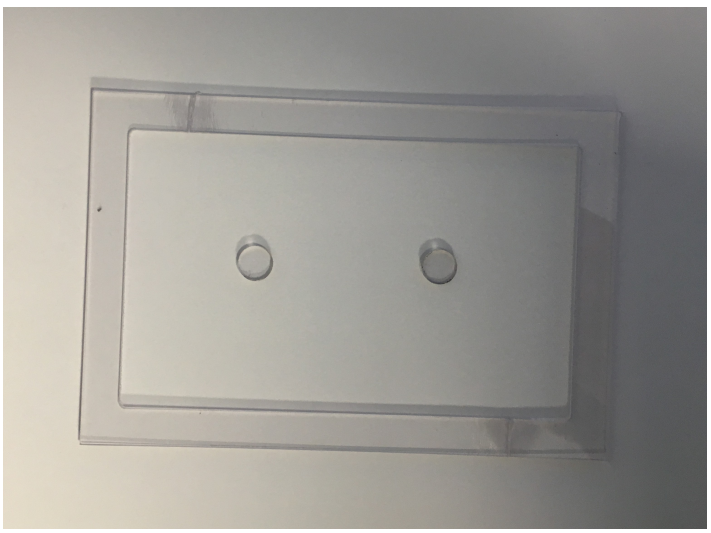

Figure 3.6. Edge and button spacers.

3.3. Formation of the Gas Gap

To form the gas gap, the spacers must be glued between the bakelite electrodes. Epoxy adhesives are widely used in RPC construction [27,28] since its main component,

resin, is the same as bakelite. We used "BISON Epoxy 5 Minutes" epoxy adhesive (Figure 3.7(a)) since its properties were suitable for our needs: super strong, suitable for many materials, chemical resistant.

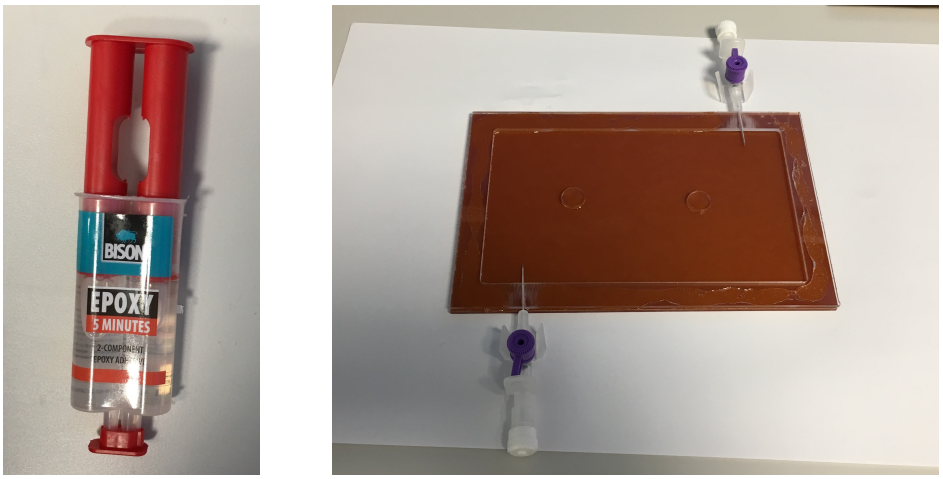

(a) Epoxy adhesive. (b) Spacers glued on one bakelite plate.

Figure 3.7. Formation of the gas gap.

First, bakelite plates and the spacers were cleaned from the dirt and dust or any residue with isopropyl alcohol then left for drying before the application of the adhesive. After they dried epoxy adhesive was applied to one side of our spacers and glued on one of the bakelite plates (Figure 3.7(b)). This adhesive starts to harden and take its shape in 5 minutes but takes its last form after a few hours. We waited for the applied adhesive to settle about 10 minutes between each step. After letting the adhesive to settle a little while another adhesive was applied to the other side of the spacers and the other bakelite plate was closed to form the gas gap. We again let it settle for a few minutes by applying pressure to the bakelite plates. Now what we needed was epoxy adhesive to harden completely to proceed to further steps. Hence, we let it harden by letting it sit overnight. To make sure the bakelite plates and the spacers are glued together strongly with minimum gap in between, we used clippers to apply pressure while the adhesive hardens (Figure 3.8). This way the adhesive spread more evenly with minimum gap in between.

After the removal of the clippers the bakelite plates and spacers were one piece and stuck very strongly (Figure 3.9). Then we applied additional few layers of adhesive

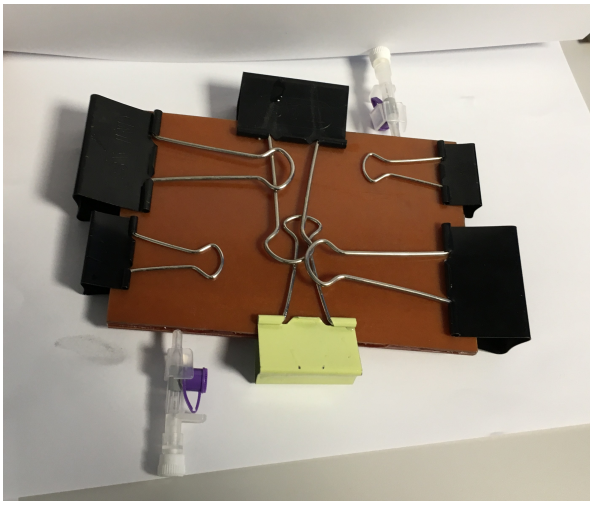

Figure 3.8. Application of pressure when the glue is hardening.

to seal the sides of the assembly, i.e. our RPC, to prevent any gaps the gas could leak from (Figure 3.10(a)). While adding layers of adhesive to the sides of our RPC we also glued our nozzles to our gas holes in order to prevent the holes from clogging (Figure 3.10(b)). To be able to proceed further, we again let it sit overnight for the adhesive to harden completely.

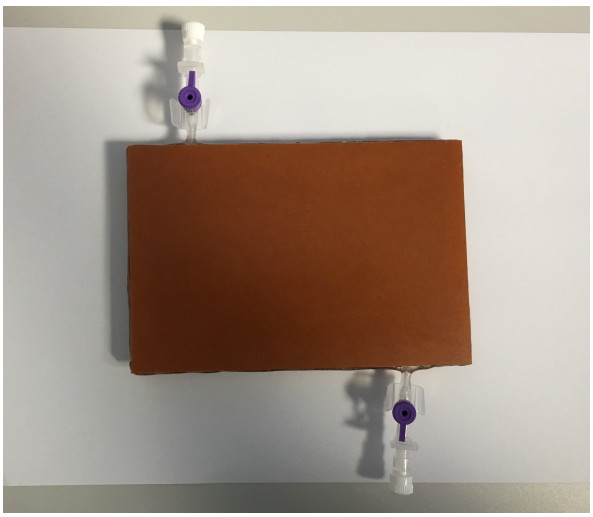

Figure 3.9. Assembly after the clippers are removed.

After our assembly was glued together with all the layers to clog any possible gaps and the glue hardened, the assembly needed to be checked for leakage. For this purpose,

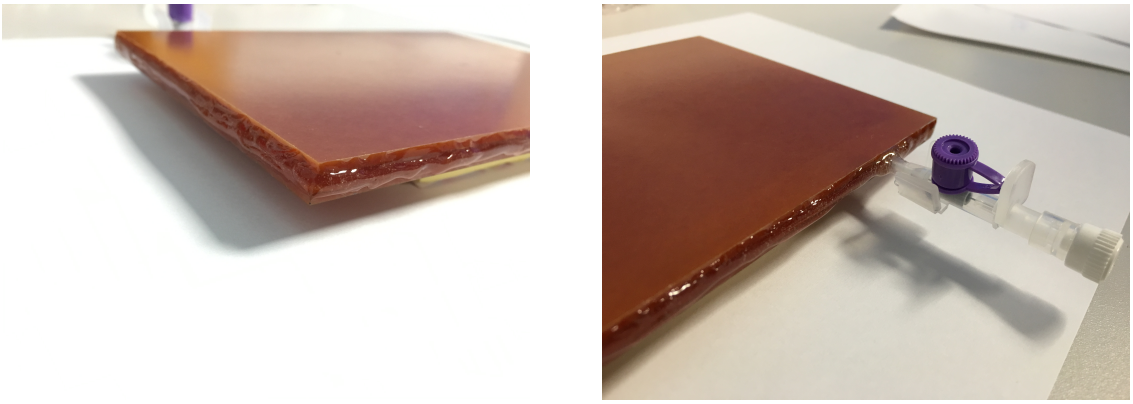

(a) Sealed sides. (b) Sealed gas nozzles.

Figure 3.10. Sealed gas gap.

we did the pressure test [29]. We checked whether the pressure inside the system stays stable over time. Stability of pressure is measured using U-Tube manometer. Our RPC had two nozzles, we used one to pump in the gas to increase the pressure inside and connected the other to the U-Tube manometer to keep track of the stability of the pressure (Figure 3.11). We did the pressure test using nitrogen gas (N_2) since it is harmless to the environment and costs less than argon gas, which will be used to run the RPC. We spotted the leakage sites using detergent water and added more layers of epoxy glue until the decrease of the pressure was negligible.

Till now we constructed the skeleton of our RPC. We separated our resistive bakelite electrodes with insulating polycarbonate spacers and formed our gas gap, the sensitive region of our RPC, where both the initial ionization due to the muons passing through and the avalanche of the electrones occur. Also we made our gas inlet and outlet. What is left out is the connection of the high voltage connectors to the system and the readout system.

3.4. Conductive Paint

A suitable conductive graphite paint for the outer surfaces of the resistive electrodes and an appropriate way to apply it to provide a uniform semi-resistive layer of graphite was needed. There were various methods of applying the graphite paint

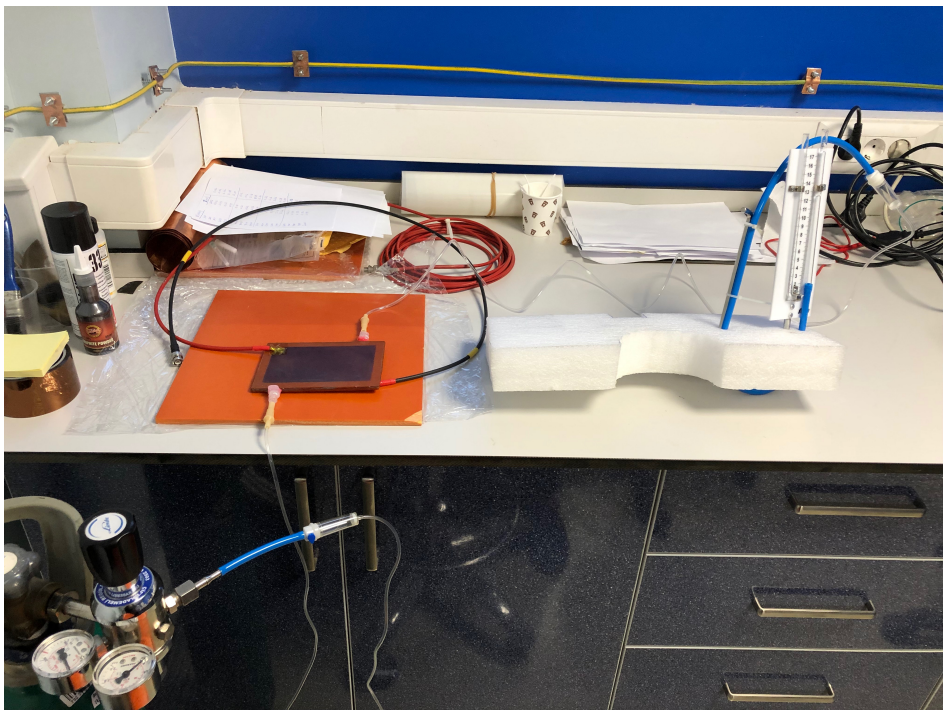

Figure 3.11. Pressure test setup.

[26, 27, 30], so we were to find the most appropriate solution for our case by trial. We needed to apply the graphite paints on the surfaces of our bakelite plates and measure the resulting surface resistivity to decide which method would be the best.

To measure the surface resistivity, a jig, which is dimensioned such that it measures resistivity per square (Equation 3.3), can be used [26, 28].

$$R = \rho\frac{l}{A} = \rho\frac{l}{l \times t} = \frac{\rho}{t} \tag{3.3}$$

where ρ is the resistivity and t is the thickness of graphite paint.

We decided to make the same jig to measure the surface resistivity. The jig was made of two conductive legs separated by insulator rods to stay in equal distance and to form a square shape (Figure 3.12). We used copper blocks in 5 cm length as the

conductive legs and two insulating epoxy rods to hold them 5 cm apart. Epoxy rods were screwed to the copper rods to fix the distance.

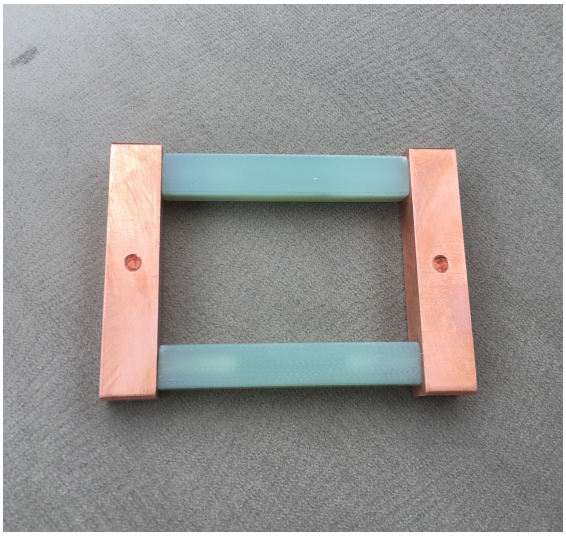

Figure 3.12. Surface resistivity measurement jig.

As the conductive graphite paint, initially there were two options, spray graphite paint and graphite powder. Since we thought spraying would produce better uniformity, we preferred to try spray graphite paint, Kontakt Chemie's GRAPHIT 33 (Figure 3.13(a)) first. We tried the paint on another surface to check if it provides conductivity on insulating materials and to try if it comes out of the surface since we were going to need to clean it from the bakelite plates if we couldn't achieve the desired values. Bakelite is a plastic-like material, so we applied the paint on a flat plastic material and achieved a uniform conductive surface. We were also able to clean the graphite paint off the surface with isopropyl alcohol, so the spray paint was suitable for repeatedly trying. Finally, we tried the paint on the bakelite plate. We sprayed it on the surface as uniformly as we could and waited overnight for it to settle. We measured the surface resistivity with our jig and found it to be on the order of 20 k$\Omega/\square$. This was highly conductive for our purposes. We seeked for resistivity around 200-300 k$\Omega/\square$ [15] or in some papers [25] around 1 M$\Omega/\square$ so we tried to decrease the amount of graphite paint we sprayed on the bakelite plate since the conductivity is proportional to the thickness of the graphite paint. However, it had a drawback. Decreasing the amount of paint caused non-uniformity. We were not able to spray the paint as we desired.

Thus, we moved on to the second option we had, graphite powder (Figure 3.13(b)). To paint with graphite powder we combined it with varnish and applied with paint brush on some plastic-like surface again to see the results of painting before trying on our bakelite plates. We chose to combine it with varnish because in [30] graphite powder was applied on the surface mixing with resin and some solvent. Varnish is made from resin so it was a good candidate and it gave our powder paint a texture that could help uniformity. This time we were also able to adjust resistivity since we could change the ratio of the graphite powder in the mixture. Biggest disadvantage of this method was that we could not remove it from the surface we applied. Since we were not able to measure the surface resistivity before applying, we had to be able to remove the graphite in case we couldn't achieve the desired order of magnitude of conductivity. Another disadvantage was that we had difficulty in applying the mixture smoothly on the surface with the brush so it was not as uniform as we expected. Some of the results of this method can be seen in Figure 3.14.

(a) Spray graphite. (b) Graphite powder.

Figure 3.13. Graphite paint options.

We then came up with another method. Since the graphite powder can be used as a paint without mixing with anything, we could also paint the surface without mixing it with varnish. It was also suitable for cleaning with isopropyl alcohol. So we tried the graphite powder paint directly on a bakelite plate by rubbing against the surface. This process was slow and more controllable than the other two methods. This way we were

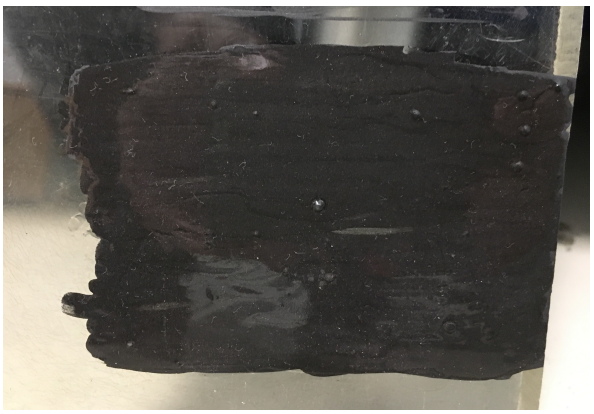

Figure 3.14. Applied graphite powder-varnish mixture.

able to adjust the conductivity by measuring between applications till the desired order of magnitude, 200-300 k$\Omega/\square$, is achieved [15]. With this method, the applied graphite also came out to be very smooth and uniform since we could control the amount of powder applied by the color the surface was turning in. Since the graphite powder was suitable for our needs we decided to use it to form the semi-conductive layer.

Before painting the surfaces, as an important precaution, the edges of the bakelite electrodes needed to be secured from the graphite paint in order to prevent any discharge that could occur from the edges. Hence, we started with securing the edges of our bakelite plates from conductive paint by applying a 1 cm width paper tape to form a frame. After securing, we painted the surfaces of our bakelite electrodes by rubbing graphite powder against the surface. Expectedly the surface got more conductive as we painted more. We checked the surface resistivity with the jig (Figure 3.15) frequently while painting to stop once the desired order of magnitude is achieved.

After we were done with painting, we took measurements of the surface resistivity for every few centimeters to calculate the average surface resistivity of each electrode. Plot of the measurements can be found in Figures 3.16(a) and 3.16(b). This plot verified that our surface resistivity is uniform enough and the desired order of resistivity is obtained on the average (253 $k\Omega$ and 319 $k\Omega$).

Figure 3.15. Measurement of the surface resistivity with the jig.

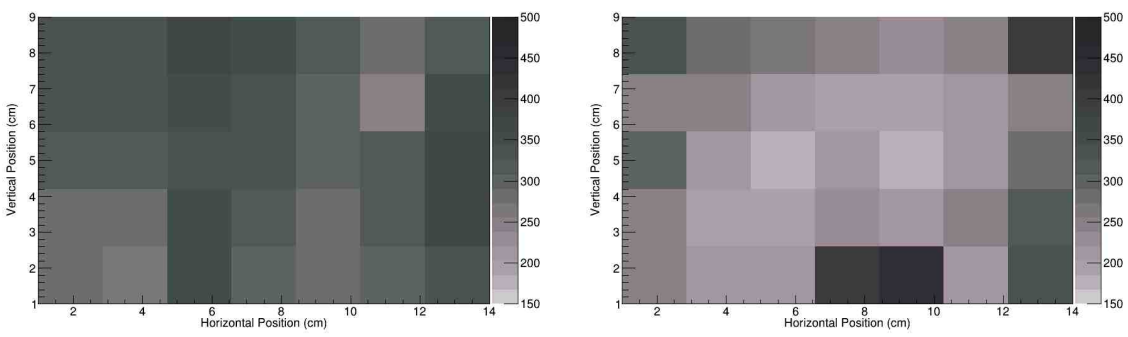

(a) Top surface. (b) Bottom surface.

Figure 3.16. Plots of the surface resistivity measurements in the units of $k\Omega/\square$.

3.5. High Voltage Connection

High voltage connection is done by soldering the HV connectors on the copper foils and pasting them on the semi-conductive surface with a kapton tape [25]. Kapton tape is used to insulate the HV connectors from the other surfaces. As in [29], we soldered our HV connectors on 1×1 cm^2 copper foils and pasted them on the opposite corners of the assembly (Figure 3.17). The upper probe was to provide the HV and the other was to be the ground. The construction of our RPC is done excluding the readout panel. Before proceeding to the construction of the readout panel, leakage current test was required to verify the insulation of the HV connectors and the whole assembly.

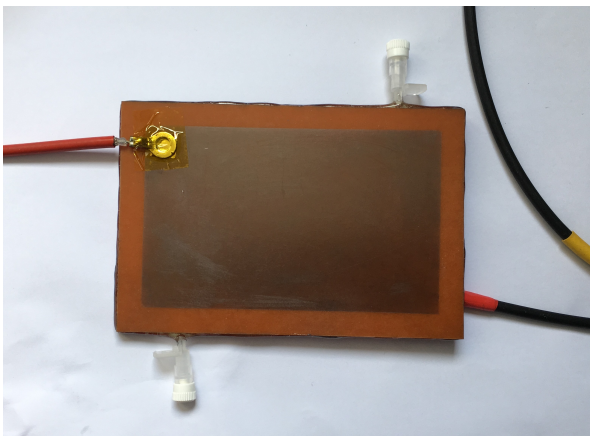

Figure 3.17. Pasted high voltage connectors.

Leakage current test is done by applying the high voltage across the electrodes and measuring the current passes through the system when the gas gap is filled with air. We increased the applied voltage up to 3000 V gradually. Voltage-leakage current curve can be seen in Figure 3.18. The maximum leakage current, corresponding to 3000 V is measured to be 0.59 mA which was a good result so our RPC was ready for the addition of the readout panel.

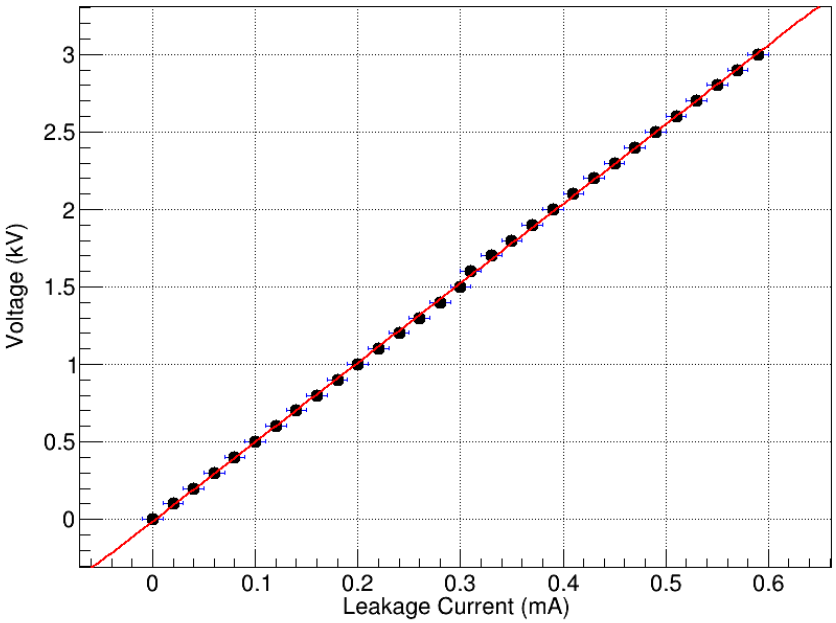

Figure 3.18. Plot of the measurements of the leakage current test.

3.6. Readout Panels

Readout signals are acquired from the copper strips which must be insulated from the high voltage connector so that the signal would not be affected. For this purpose 200-300 μm thick insulating Mylar sheets are used [1]. We obtained a 250 μm thick Dupont Mylar sheet from its Turkish distributor, Emtel Emaye.

For the signal readout part, construction steps are as follows. First step is gluing the insulating Mylar sheet on the graphite coated surface. Then, the readout strips are pasted on the Mylar sheet above the graphite coated area. To connect the strips to the front-end electronics, ribbon cables are soldered on the strips [1]. This concludes what needs to be done with the readout part.

There are two different approaches for the signal readout. The signal can be obtained from only one side which gives a one dimensional position information or it can be obtained from both sides, which gives a two dimensional position information

with the perpendicularly placed readout strips on the opposite surfaces. We decided to design our RPC to have the readout panels on both sides. 15 mm thick copper strips, 9 cm in length on one side and 14 cm in length on the other side, were used. The gap between each strip was chosen to be around 2 mm [27]. To approximately fit them above the graphite coated area, 5 copper strips on one side and 8 copper strips on the other side were used. While constructing the readout part we also decided to work off the surface of the RPC to not damage the finished part.

We cut two 10×15 cm^2 rectangles from our Mylar Sheet since we needed to cover both the top and the bottom surfaces of our RPC. We cleaned our insulating sheets with isopropyl alcohol and let them dry. Then we cut the properly sized pieces from the copper tape to be the readout strips. To connect the copper strips to the readout electronics, we used ribbon cables.

We first started with soldering the ribbon cables on the copper strips. This way, if anything unexpected happens the Mylar sheets wouldn't be damaged. Then we pasted the strips on the Mylar sheets while trying to keep the distance between each strip around 2 mm. The readout panels were ready to be joined to the RPC (Figure 3.19).

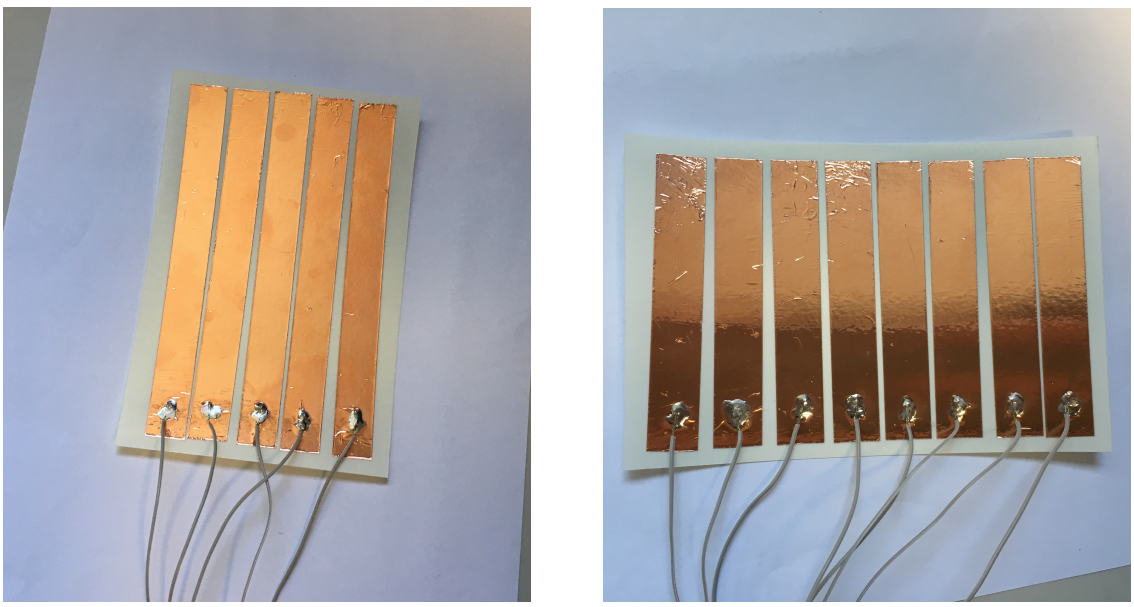

(a) Top panels. (b) Bottom panels.

Figure 3.19. Readout panels.

For the combining process instead of using the general approach, which is gluing the readout panels to the assembly, we used kapton tape. Initially, we placed the readout panels, one to the upper surface and one to the lower surface. Then, we secured the whole assembly together with kapton tape from the sides to make them stay together as one unit (Figure 3.20). This approach provided us with two main benefits. First, since the tape can be easily removed, the readout panels can be replaced with new ones depending on the needs. Second, the graphite coated surface can also be reached easily, therefore the conductivity can be adjusted for various purposes, e.g. to measure its effect on efficiency, spatial resolution and so on. This was the final step of the readout part and also of the construction of the RPC.

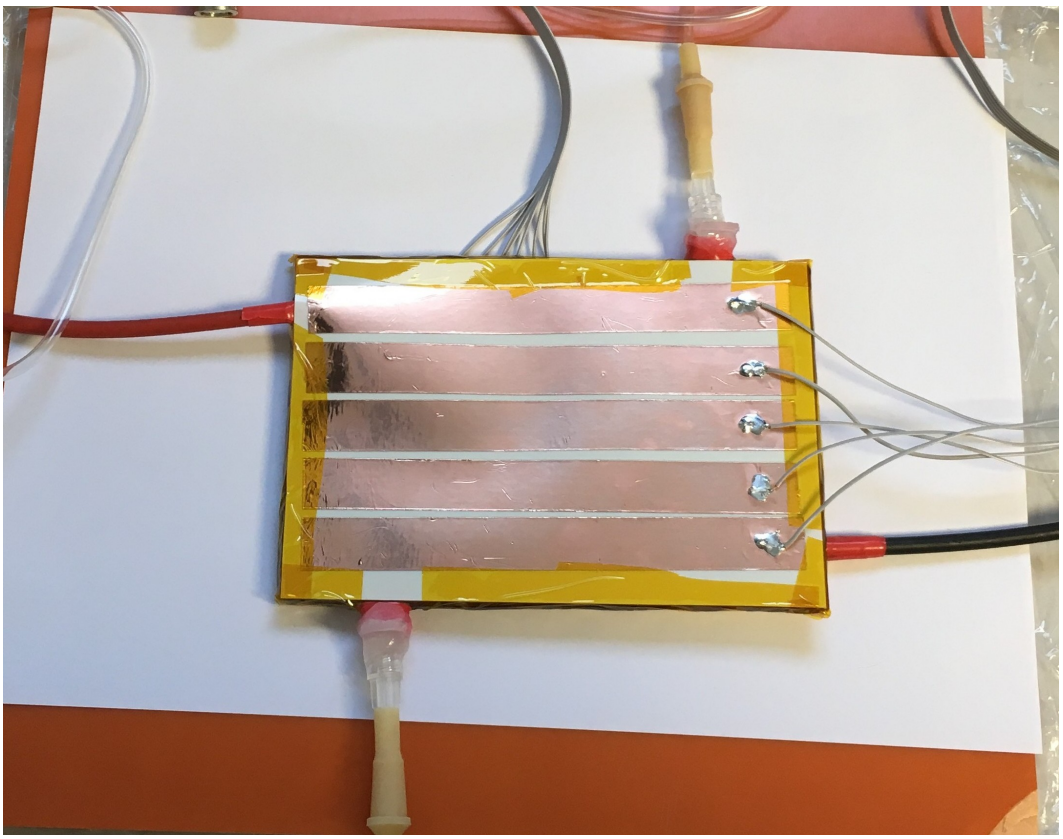

(a) Top side.

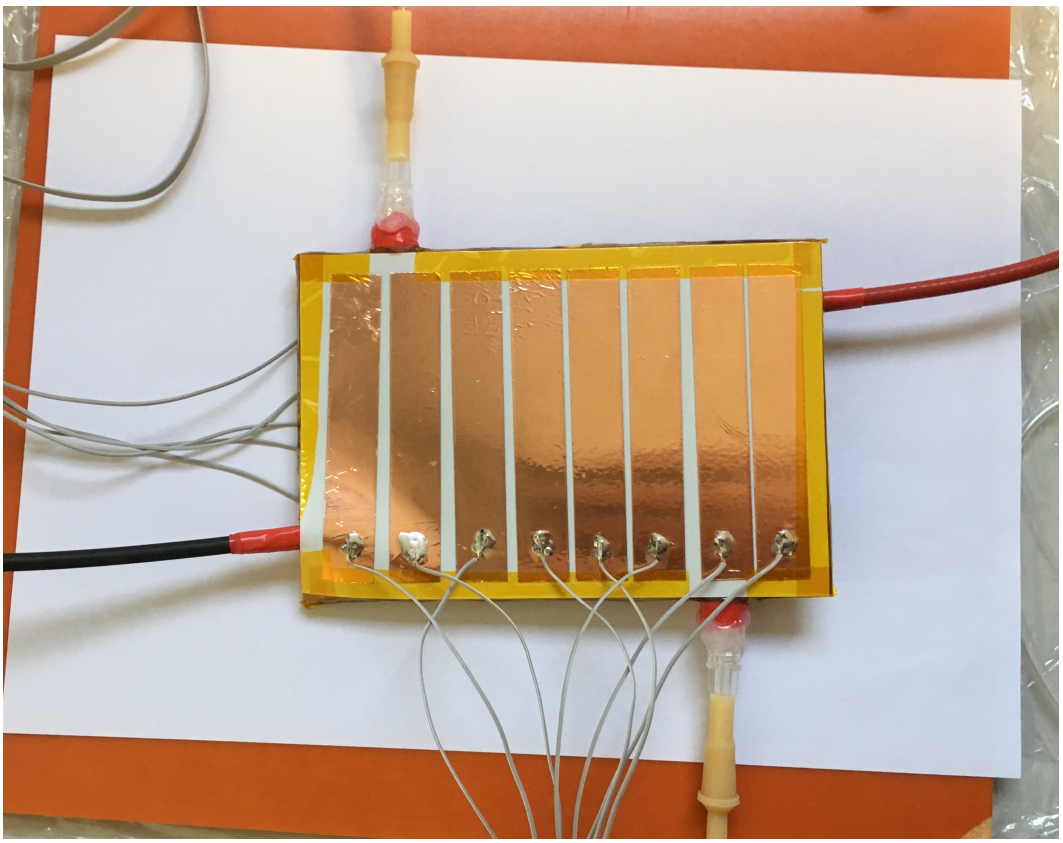

(b) Bottom side.

Figure 3.20. Completed RPC prototype.

4. DATA ACQUISITION

To read the induced signals, readout panels are connected to ground through 50 Ω resistances and the voltage across them is read by an oscilloscope. The data acquisition circuit can be seen in Figure 4.1. Considering the same assumption where the electrons drift towards the lower copper strips, a current coming from ground to the lower strips is induced. Hence, a negative voltage on the 50 Ω resistance must be read from the oscilloscope. As explained before, since the situation is reversed for the upper strips, a positive voltage is induced on the other 50 Ω resistance that was connected to the upper readout panel. Thus, a signal that has an almost identical but reversed shape must be observed.

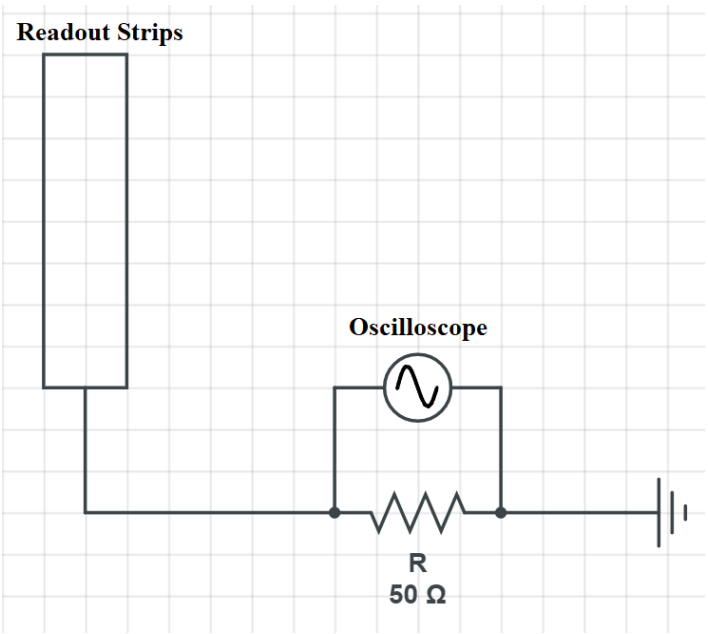

Figure 4.1. Data acquisition circuit.

After connecting the readout panels to the oscilloscope, high voltage connectors of the RPC are connected to the high voltage source. Also the gas inlet is connected to the gas tank for the gas pump. Our system is in Figure 4.2. The data are taken with the gas gap filled with air, pure argon, pure isobutane and intermediate mixtures.

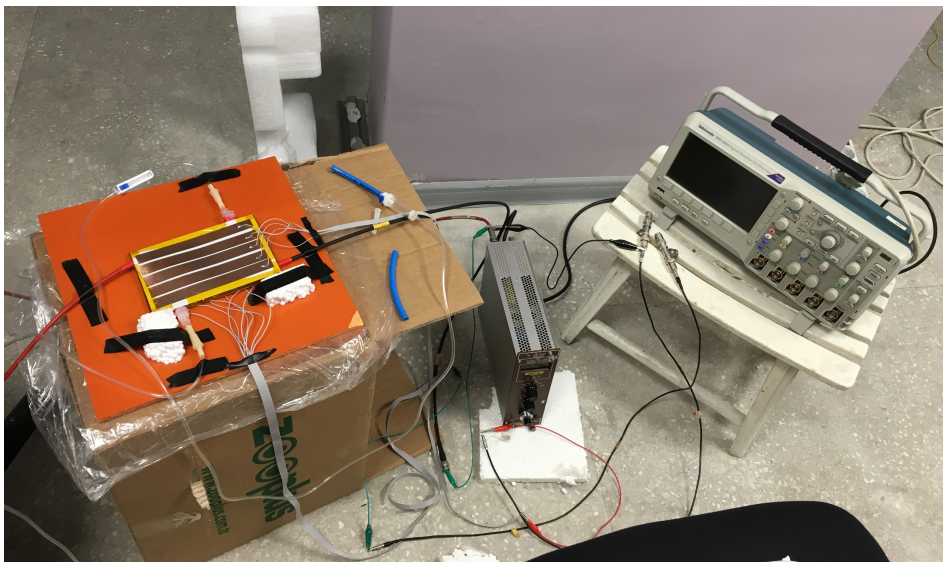

Figure 4.2. Data acquisition setup.

4.1. Observations

Observations are made by examining the signal behavior and comparing the signal rates with different applied voltages for different gases. Also, the signal behavior while changing the gas mixture is observed. These observations are done with a high voltage source that can provide up to 3000 V.

4.1.1. Observations With Air

Initially, we tested the RPC with air before trying other gases. Signal rates and their alteration with the varied voltage is observed and recorded. For this, first the minimum voltage level that a signal can be observed is determined. Then, number of signals are counted for 3-minute intervals for increasing voltage levels (Figure 4.3). Increase of the signal rates with the increased voltage is observed. We used two different trigger levels, 8 mV and 20 mV, to compare signal rates with different signal sizes and their comparison can be seen in Figure 4.4.

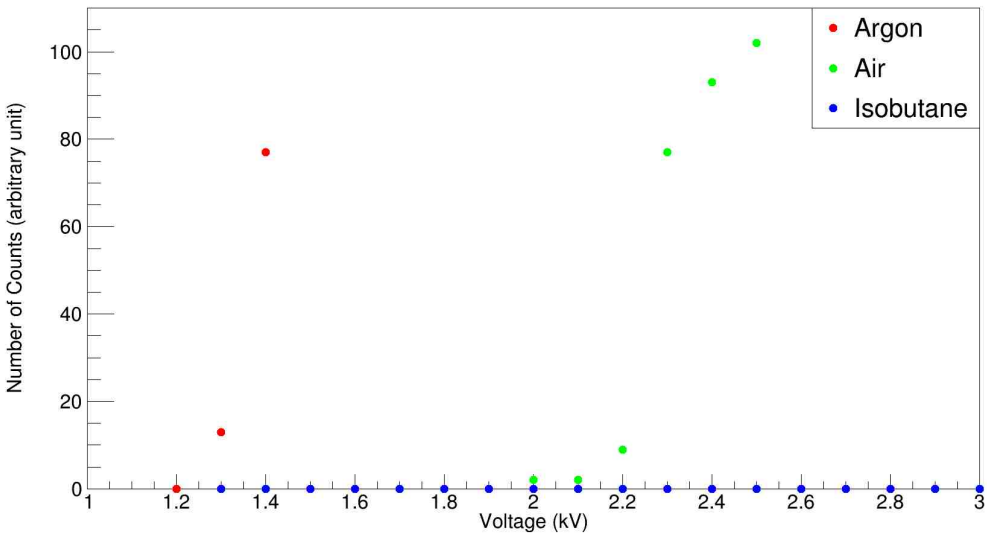

Figure 4.3. Count test for argon, air and isobutane at 20 mV trigger level for 3-minute intervals.

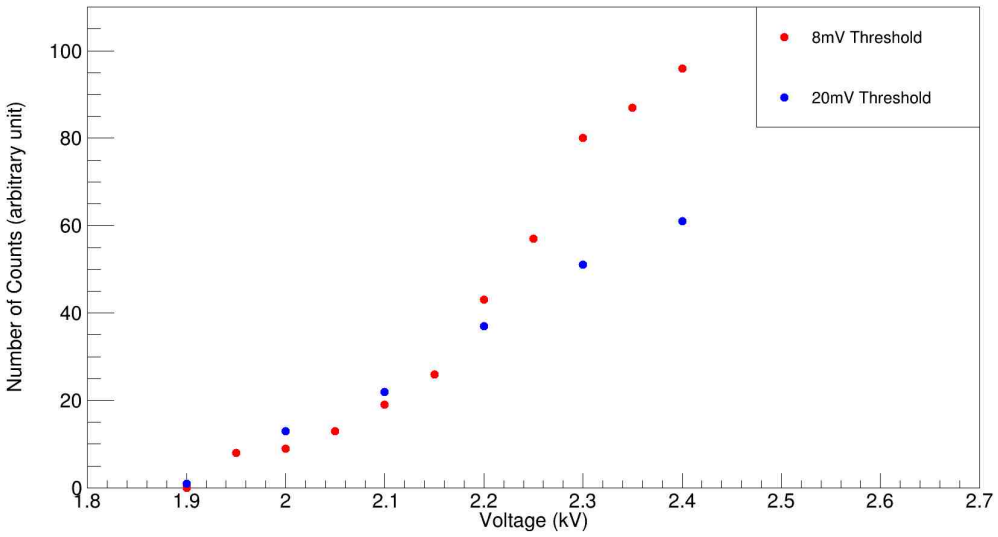

Figure 4.4. Count test for air with two different trigger thresholds for 3-minute intervals.

4.1.2. Observations With Argon

To test the RPC with argon, pure argon is pumped slowly into the gas gap. While the argon was flowing into the gap, we observed the signal behavior at a constant voltage. Signal rates increased very rapidly. After the sufficient amount of gas flow is ensured, same procedure that was applied with air is done with argon. With the pure argon, very frequent signals were observed at the voltage level, 1900 V, where we almost did not see any signal operating with air. Signal rates were observed and recorded. Comparison of the count rates of argon with air can be seen in Figure 4.3. Significant amount of increase in the signal rates compared to the air is observed. As in the case of air, signal rates increased with the increasing voltage.

Another observation was that when operating with argon, signals started at lower voltage levels and became too rapid to count with the eye at relatively low voltage levels. Hence, the count test we did with the air was deficient. However, the signal frequency was so high that oscilloscope could provide us with signal frequency. Signal rate-applied voltage characteristics for argon at relatively high voltages can be seen Figure 4.5.

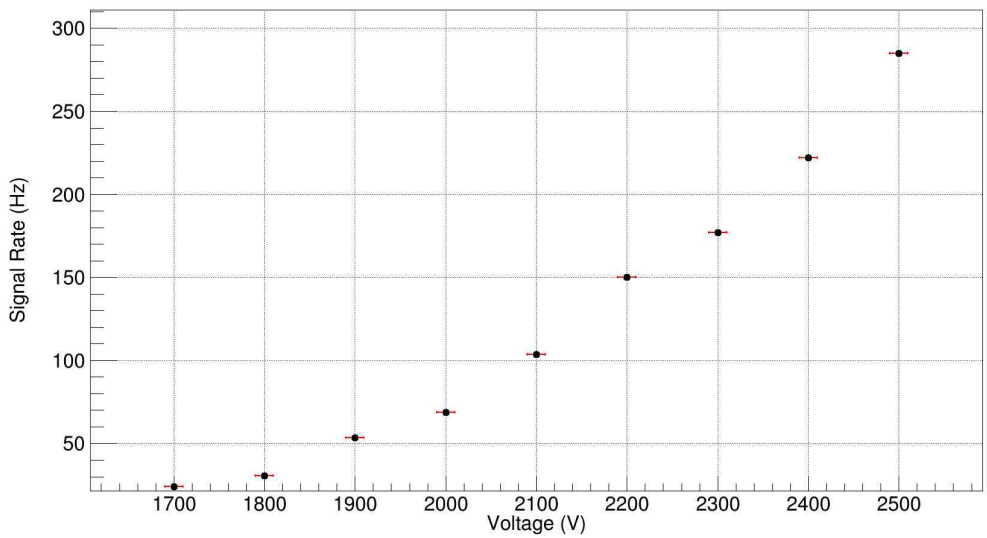

Figure 4.5. Signal rates for argon at relatively high voltages.

4.1.3. Observations With Isobutane and Intermediate Mixtures

Since RPCs are operated with the presence of UV absorber gases in the gas mixture and the first prototype was also operated with the argon and isobutane gas mixture, we wanted to see the behavior of our RPC's operation with pure isobutane and also with the mixture of argon and isobutane.

First we tested the RPC with pure isobutane and no signal was observed up to the limit of our HV source (Figure 4.3). Then, since there were no available gas mixing units and the gas flow rate was uncontrollable we proceeded to examine the change in the signal rate as we slowly pumped in isobutane when the gap was filled with argon at a constant voltage. After isobutane started to flow inside the gas gap very rapid signals fade away in a small amount of time.

In the reverse case, pumping in argon when the gas gap was filled with isobutane, first with the presence of the isobutane no signals were seen even at the highest voltage level we could provide. Then argon was slowly flowed inside the gas gap. After a few minutes signals started to developed. When the signals were frequent we decreased the applied voltage to avoid the plasma formation so that we could obtain more valuable signals. With the decrease of the voltage signals were lost for a few minutes and then developed again. With every step the same sequence was observed.

4.2. Discussion

The results obtained from the preliminary tests are promising for various reasons. First of all, the induced signals from upper and lower readout strips are reversed in shape, which implies a gas discharge. In addition, signal rate increases with increasing voltage which is also compatible with gas discharge theory. These two characteristics was common for all the gases we tried, which is also expected.

The tests with argon and isobutane are also compatible with the theory. The signal rate increases rapidly for pure argon and reaches very high values which indicates

the formation of plasma (Figure 4.6) and it is known that pure argon forms plasma under the effect of high voltages. Even a small fraction of added isobutane decreases the signal rate to a large extend expectedly, since isobutane is a UV absorber gas that is commonly used in RPCs to avoid photoionization as explained earlier.

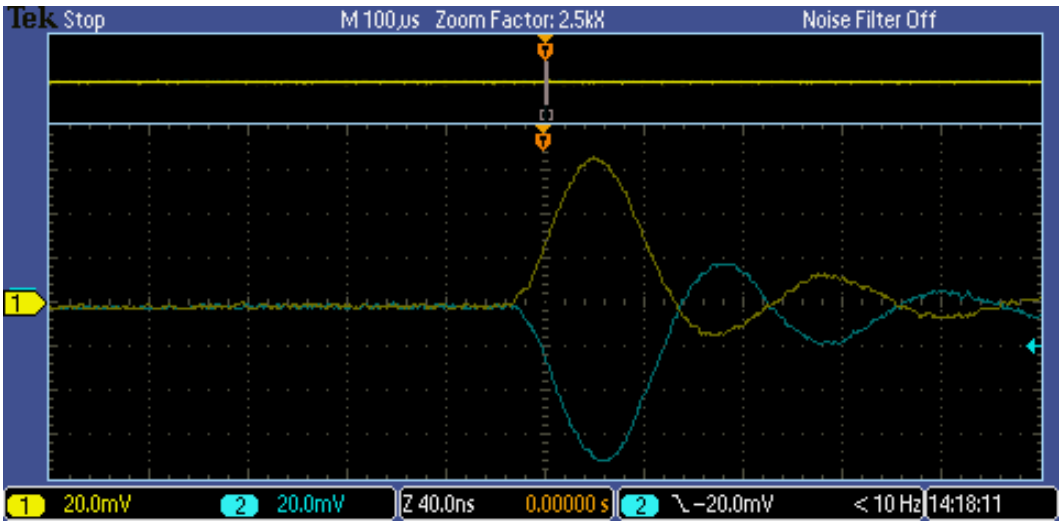

(a) 1400 V.

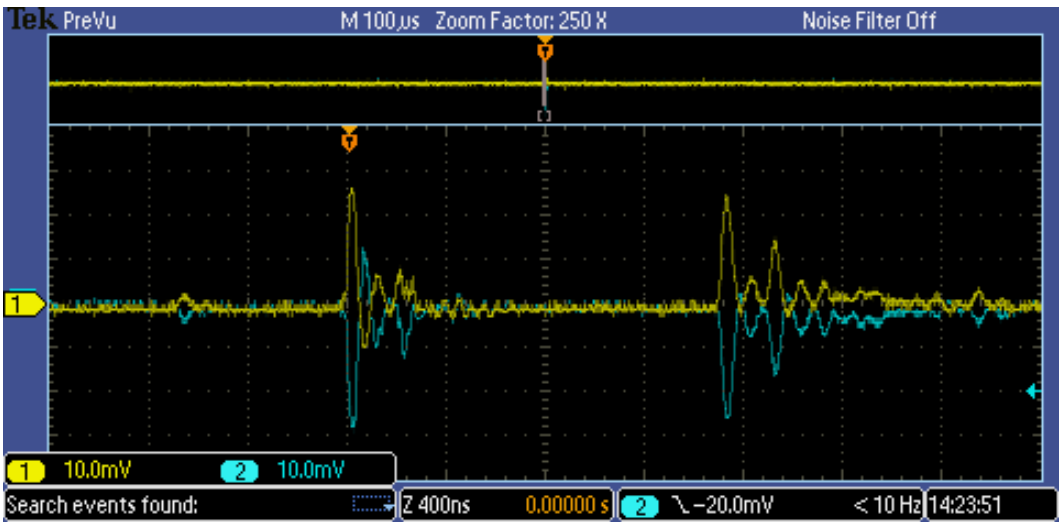

(b) 1900 V.

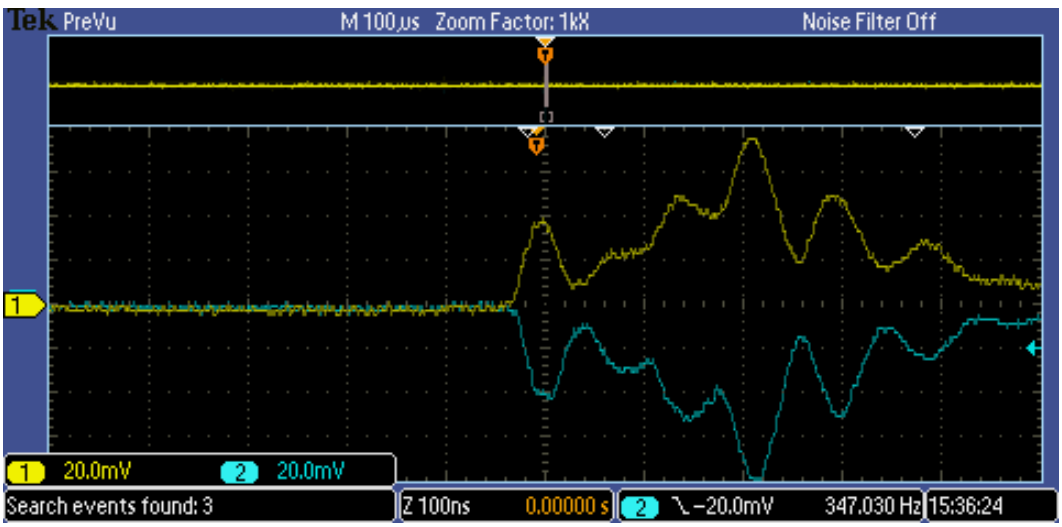

(c) 2500 V.

Figure 4.6. Example signals with argon at different voltage levels.

5. CONCLUSION

Resistive plate chambers (RPCs) play critical roles in the particle detectors at CERN, as they detect and measure particles as muons and provide crucial input to the trigger systems. They are likely to be essential for any collider experiments that will be built in the future. Unfortunately, to the best of our knowledge, no attempts for constructing RPCs in Turkey has been made before and this thesis presents the very first RPC prototype built in Turkey.

This prototype has been built with very limited budget and resources. Along the way, we have come up with many improvisational techniques to overcome the unavailability of various conventional methods. In addition, valuable knowhow about the construction steps and domestic availability of the materials used have been obtained. All the materials, except the bakelite plates, have been procured domestically. This thesis itself has been formulated to function as a detailed construction manual for anyone planning to build an RPC, as we have found such a detailed resource missing in the literature. A substantial effort has been made to present the construction steps in utmost detail together with supplementary photographs.

The observed electrical signals, as we believe, are due to ionization processes occurring in the gas mixture caused by the applied high voltage. In addition, signal behavior with the changing gases under the influence of varying high voltage has also been found to be in agreement with theoretical expectations. To obtain further information about the source of the signals, RPCs can be tested in coincidence with scintillators. Such tests, as well as a detailed simulation of the constructed detector are planned for a future study. In addition, since the gas mixture is crucial to evaluate the real performance of the RPC, further tests can be done with a proper gas mixing unit.

In summary, we have presented a very modest RPC that has been built by two MSc students, my coworker and I, with no prior experience and almost no outside

assistance, to be the pioneering work in the construction of RPCs in Turkey. While it is modest, we believe that it will provide a basis for securing the project grants to construct in Turkey RPCs with tens of square meters in area to be used in future upgrades of the ATLAS detector at CERN.

REFERENCES

1. Abbrescia, M., V. Peskov and P. Fonte, *Resistive Gaseous Detectors*, Wiley-VCH Verlag GmbH and Co. KGaA, Boschstr. 12, 69469 Weinheim, Germany, 2018.

2. Santonico, R. and R. Cardarelli, "Development of resistive plate counters", *Nuclear Instruments and Methods in Physics Research*, Vol. 187, pp. 377–380, 08 1981.

3. Lippmann, C., *Detector Physics of Resistive Plate Chambers*, Ph.D. Thesis, Frankfurt U., 2003.

4. Riegler, W., *Particle Detectors*, 2007, `https://indico.cern.ch/event/431965/attachments/936633/1327138/L5_riegler.pdf`, accessed at May 2019.

5. Keuffel, J. W., "Parallel-plate counters and the measurement of very small time intervals", *Phys. Rev.*, Vol. 73, p. 531, 1948.

6. Keuffel, J. W., "Parallel-plate counters", *Rev. Sci. Instrum.*, Vol. 20, p. 202, 1949.

7. Charpak, G. and F. Sauli, "The multistep avalanche chamber: A new high-rate, high-accuracy gaseous detector", *Physics Letters B*, Vol. 78, 10 1978.

8. Babykin, M. V., A. G. Plakhov, Y. F. Skachkov and V. V. Shapkin, "Plane-parallel spark counters for the measurement of small times", *The Soviet Journal of Atomic Energy*, Vol. 1, pp. 487–494, 1956.

9. Parkhomchuck, V., Y. Pestov and N. Petrovykh, "A spark counter with large area", *Nuclear Instruments and Methods*, Vol. 93, No. 2, pp. 269 – 270, 1971, `http://www.sciencedirect.com/science/article/pii/0029554X71904757`.

10. Schmidt, H. R., "Pestov spark counters: Work principle and applications", *Nuclear Physics B-proceedings Supplements*, Vol. 78, pp. 372–380, 08 1999.

11. Pestov, Y. N. and G. V. Fedotovich, "A Picosecond Time-of-flight Spectrometer For The Vepp-2m Based On Local - Discharge Spark Counter", *Slac Translation*, Vol. 184, pp. 77–78, 1978.

12. Cattani, G., "The Resistive Plate Chambers of the ATLAS experiment: performance studies", *Journal of Physics: Conference Series*, Vol. 280, 02 2011.

13. Ying, J., Y. L. Ye, Y. Ban, H. T. Liu, Z. M. Zhu, Z. Y. Zhu, T. Chen, J. G. Ma and S. J. Qian, "Study of an avalanche-mode resistive plate chamber", *Journal of Physics G: Nuclear and Particle Physics*, Vol. 26, No. 8, pp. 1291–1298, 07 2000,

14. Cardarelli, R. and R. Santonico, *High resolution timing for muon detectors at future colliders*, `https://indico.cern.ch/event/358198/contributions/849873/attachments/713325/979297High_time_resolution.pdf`, accessed at June 2019.

15. Cardarelli, R., R. Santonico, A. Di Biagio and A. Lucci, "Progress in resistive plate counters", *Nuclear Instruments and Methods in Physics Research Section A: Accelerators, Spectrometers, Detectors and Associated Equipment*, Vol. 263, pp. 20–25, 01 1988.

16. Abbrescia, M., L. Benussi, D. Piccolo, S. Bianco, M. Ferrini, S. Muhammad, L. Passamonti, D. Pierluigi, D. Piccolo, F. Primavera, A. Russo and G. Saviano, "Eco-friendly gas mixtures for Resistive Plate Chambers based on tetrafluoropropene and Helium", *Journal of Instrumentation*, Vol. 11, No. 08, pp. P08019–P08019, aug 2016,

17. Guida, R., B. Mandelli and G. Rigoletti, "Performance studies of RPC detectors with new environmentally friendly gas mixtures in presence of LHC-like radiation background", *Nuclear Instruments and Methods in Physics Research Section A: Accelerators, Spectrometers, Detectors and Associated Equipment*, 2019, `http://www.sciencedirect.com/science/article/pii/S0168900219304759`.

18. Agrigoroae, C., *A "muoscope" with CMS technology*, https://home.cern/news/news/knowledge-sharing/muoscope-cms-technology, accessed at June 2019.

19. Townsend, J. S., "The Conductivity produced in Gases by the Motion of Negatively-charged Ions", *Nature*, Vol. 62, No. 1606, pp. 340–341, 1900, https://doi.org/10.1038/062340b0.

20. Raether, H., *Electron avalanches and breakdown in gases*, Butterworths advanced physics series, Butterworths, London, 1964, https://cds.cern.ch/record/102989.

21. Fonte, P. *et al.*, "Feedback and break-down in parallel plate chambers", *Nuclear Instruments and Methods in Physics Research*, Vol. 305, pp. 91–110, 1991a.

22. Davies, A. J. and C. J. Evans, *The theory of ionization growth in gases under pulsed and static fields*, CERN Yellow Reports: Monographs, CERN, Geneva, 1973, https://cds.cern.ch/record/186263.

23. Shockley, W., "Currents to Conductors Induced by a Moving Point Charge", *Journal of Applied Physics*, Vol. 9, pp. 635–636, 10 1938.

24. Ramo, S., "Currents induced by electron motion", *Proc. Ire.*, Vol. 27, pp. 584–585, 1939.

25. Biswas, S., *Development of High Resolution Gas Filled Detector for High Energy Physics Experiments*, Ph.D. Thesis, University of Calcutta Department of Physics, 2010.

26. Neog, H. *et al.*, "Building of a Bakelite Resistive Plate Chamber prototype", *XXI DAE-BRNS High Energy Physics Symposium*, 2014.

27. Biswas, S., S. Bhattacharya, S. Bose, S. Chattopadhyay, S. Saha, M. K. Sharan

and Y. P. Viyogi, *Development of bakelite based Resistive Plate Chambers*, 2008.

28. Shinde, R. R. and E. Yuvaraj, *Fabrication and Characterization of Glass Resistive Plate Chamber (RPC)*, Tech. rep.

29. Neog, H., "Building of a Bakelite Resistive Plate Chamber Detector", *Student Journal of Physics*, Vol. 6, 2017.

30. Vanheule, S., *Design of a glass resistive plate chamber for the upgrade of the Compact Muon Solenoid muon system*, Master's Thesis, Universiteit Gent Faculteit Wetenschappen Vakgroep Fysica en Sterrenkunde, 2013.